Electronic structure analysis of α-SiO_2 via x-ray absorption near-edge structure at the Si K, $L_{2,3}$ and O K edges

1998 J. Phys.: Condens. Matter 10 8083

(http://iopscience.iop.org/0953-8984/10/36/016)

J. Phys.: Condens. Matter **10** (1998) 8083–8092. Printed in the UK PII: S0953-8984(98)93216-7

Electronic structure analysis of α-SiO_2 via x-ray absorption near-edge structure at the Si K, $L_{2,3}$ and O K edges

Z Y Wu†‡, F Jollet† and F Seifert§

† Commissariat à l'Energie Atomique, DSM/DRECAM/SRSIM, Bâtiment 462, CE Saclay, 91191 Gif-sur-Yvette Cédex, France

‡ Istituto Nazionale di Fisica Nucleare, Laboratori Nazionali di Frascati, PO Box 13, 00044 Frascati, Italy

§ Bayerisches Geoinstitut, Universität Bayreuth, D-95440 Bayreuth, Germany

Received 7 April 1998, in final form 22 June 1998

Abstract. The electronic structure of empty states in quartz (α-SiO_2) has been investigated by calculating the individual contributions of Si 1s, 2p and O 1s to the x-ray absorption near-edge structure (XANES) spectra; excellent agreement has been found between the experimental data and full multiple-scattering calculations. On the basis of the comparison, the origins of the spectral transition features can be assigned unambiguously. Although symmetry-based molecular-orbital theory is qualitatively adequate for describing these spectra, the interpretation of the Si K-edge XANES spectrum exclusively in terms of a ground-state potential is inappropriate in general.

1. Introduction

Quartz (α-SiO_2) is an interesting insulator material with a wide range of applications such as in optoelectronics, high precision scale time bases, and metal oxide semiconductor devices. Recently, its valence band has been extensively studied both theoretically and experimentally by using photoelectron spectra (x-ray (XPS) or ultraviolet (UPS)) and x-ray emission spectra (XES) [1–11]. However, its conduction band structure and the unoccupied density of states (DOS) are not very well understood mainly due to theoretical limitations and experimental difficulties in the soft-x-ray region. Only a few experimental studies have been reported, and no detailed quantitative agreement between experiment and theory has yet been achieved [12–20].

X-ray absorption near-edge structure (XANES) can provide directly information on the unoccupied electronic states of solids. It is a local process in which a core electron is excited to an unoccupied state in the initial, unperturbed state of the system. In a first-order approximation, for instance, neglecting the core-hole potential effect, the one-electron cross section may be decomposed into a product of an energy-dependent matrix element overlap factor $M(E)$ and a projected density of states $\rho(E)$ with appropriate symmetry, $\sigma(E) \propto M(E)\rho(E)$ [21, 22]. The near-edge structure is expected to reflect the DOS of the conduction band, provided that the matrix element $M(E)$ is slowly varying in that energy region.

In previous band-structure calculations, Fowler *et al* [23] presented only the total DOS; comparison between theoretical and experimental spectra is difficult. Jollet and Noguera [24] used two different methods to calculate the conduction band DOS: a self-consistent

0953-8984/98/368083+10$19.50

band-structure calculation and a self-consistent embedded-cluster calculation which allows one to include the effect of the core hole. By using the second method, they found that the calculated p DOS on an excited silicon atom compares satisfactorily with the experimental spectrum. In contrast, Tanaka *et al* [25] presented the results of a first-principles molecular-orbital calculation for three forms of silicon dioxide by using the discrete variational (DV) X_α method. They claimed that the partial DOS in the ground state agrees well with the fine structure of the experimental XANES in the range $\leqslant$30 eV. Very recently, Briois *et al* [26], Chaboy *et al* [27], and Wu *et al* [28] tried to simulate all of the XANES data for α-SiO_2 by means of a multiple-scattering (MS) approach with various potentials and increasing size of atomic clusters, but their computations fail to give good energy separations and the correct relative intensities of some transition peaks. The origin of some transition features in the experimental spectra has not been explained in these papers. Even so, the role of the core-hole potential for the experimental data has been emphasized in these papers.

Detailed studies on the electronic structure of α-SiO_2 have produced some conflicting conclusions. In order to bring new arguments into this discussion and shed light on the type of transition involved, we present in this paper experimental data and *ab initio* full MS calculations of the XANES spectra at the Si K, $L_{2,3}$ and O K edges for α-SiO_2. In this way we try to connect the spectral features with the atomic arrangement, the unoccupied DOS, and the ligand-field characters, and to establish the origin of the transition features.

2. Experiments

α-SiO_2 has been prepared as described in reference [29]. Its structure consists of an ordered trigonal lattice of interconnected SiO_4 tetrahedra, with lattice constants $a_0 = 4.913$ Å and $c_0 = 5.404$ Å. The SiO_4 tetrahedron is not quite regular, with two different Si–O distances of 1.5951 and 1.6167 Å; the intra-tetrahedral O–Si–O angle is about 109°, and the inter-tetrahedral Si–O–Si angle is about 144°. The c-axis (chosen to lie along the z-axis) is a threefold axis. The atomic clusters each have C_2 symmetry for the Si sites and no symmetry for the O sites.

X-ray absorption spectroscopy (XAS) experiments were carried out at the SuperAco synchrotron radiation source (Laboratoire pour l'Utilisation du Rayonnement Electromagnetique—LURE, Orsay, France). The silicon K-edge absorption spectra were recorded on the SA32 line. The monochromator was 'two-parallel-crystal'-type InSb, with diffracting surfaces cut parallel to the (111) plane. The photon energies ranged from 1500 to 2500 keV, with a resolution of 0.7 eV. The Si L-edge spectrum is from reference [16].

The oxygen K-edge absorption spectrum was recorded on the SA72 line. The monochromator was a TGM 10 m toroidal grating mirror. The photon energies ranged from 150 to 1500 eV, with a resolution of 0.5 eV. More details can be found in reference [28].

3. Calculational details

The XANES spectra have been computed using full MS theory and programs described elsewhere [30–36]. In the muffin-tin model and one-electron approximation, the local density potential for the system can be constructed on the basis of the Mattheiss prescription [37] by superposition of neutral atomic charge densities using the Clementi–Roetti basis-set tables [38]. For the exchange–correlation part of the potential, for practical reasons, we use the energy-independent X_α potential with α equal to 0.99 for excited Si atoms and 0.744 for oxygen. In order to simulate the charge relaxation around the core hole, we use the

well tested screened $(Z + 1)$-approximation final-state rule [34] which consists in taking into account the orbitals of the $Z + 1$ atom, and constructing the charge density by using the excited electronic configuration of the photoabsorber with the core electron promoted to an empty orbital. The subsequent solution of the effective Schrödinger equation for the final state is then straightforward. The calculated spectra are further convoluted with a Lorentzian-shaped function with a full width of Γ_h [39] to account for the core-hole lifetime and Γ_{exp} to account for the experimental resolution. We have chosen the muffin-tin radii according to the Norman criterion [40] and allowed a 15% overlap between contiguous spheres to simulate the atomic bond and to minimize the potential discontinuities [41]. The z-axis is along the c-axis of the compound in all of our calculations.

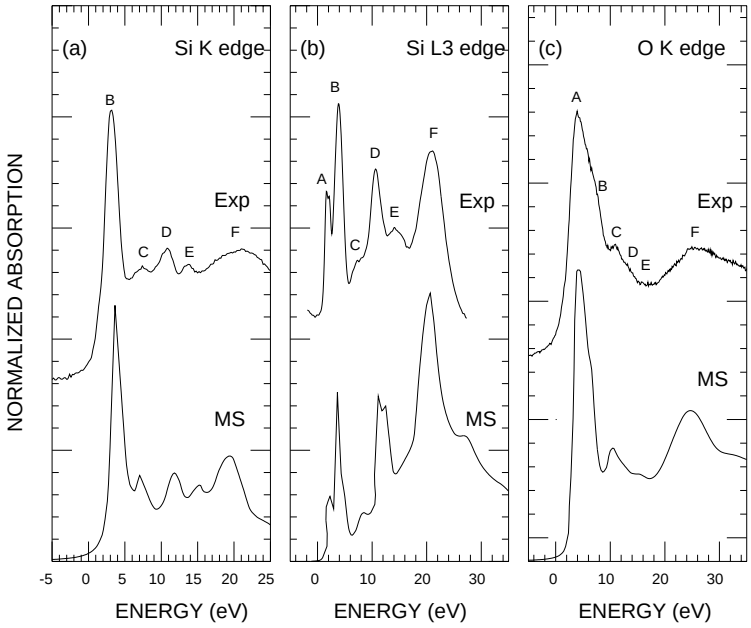

Figure 1. Experimental ('Exp') and multiple-scattering ('MS') calculated XANES spectra of α-SiO$_2$: the Si K edge (left-hand panel), Si L$_{2,3}$ edge (middle panel), and O K edge (right-hand panel).

4. Results and discussion

Figure 1 shows the experimental Si K-, Si L$_{2,3}$-, and O K-edge XANES spectra of α-SiO$_2$, along with the calculated MS results. All of these spectra display several main spectral features (labelled A, B, C, D, E, and F), and they are in good agreement with other published work [16, 17, 29, 42, 43]. In the MS theoretical computations the size convergence was obtained using a cluster of 109 atoms for the Si K-edge spectra, 57 atoms for the Si L$_{2,3}$-edge spectra, and 80 atoms for the O K-edge spectra.

4.1. The Si K edge

The Si K-edge XANES spectrum is presented in figure 1(a). It consists of a strong line, the so-called 'white line' (labelled B), followed by four structures C, D, E, and F. With

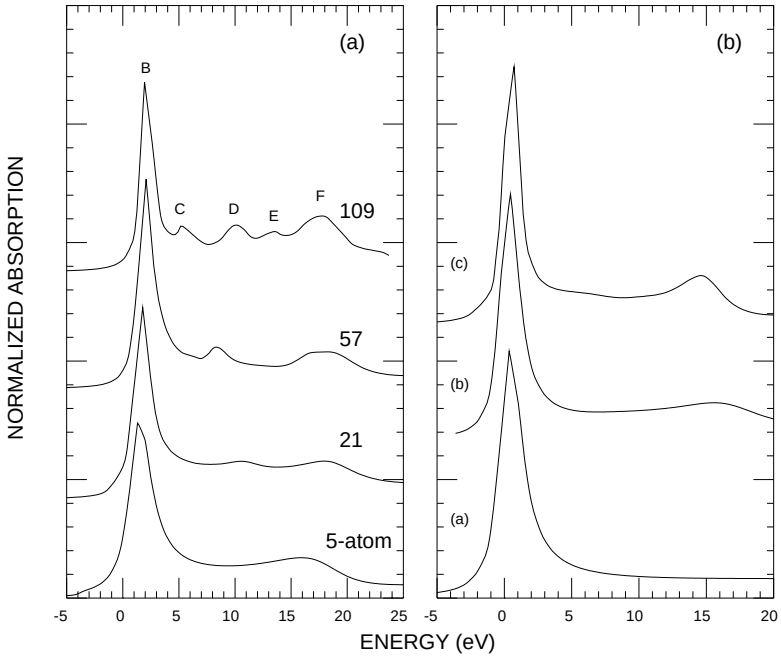

Figure 2. Panel (a): theoretical XANES spectra taken at the Si K edge for α-SiO_2 for various cluster sizes (5, 21, 57, and 109 atoms). Panel (b): (a) the 5-atom-cluster calculation, but with the d-like bases of the central Si atom suppressed; peak F has disappeared, indicating that this peak arises from a dipole-allowed 1s-to-3d (T_2(d)) state transition; (b) the 9-atom (central $Si + 4O + 4Si$) MS calculation; (c) the 17-atom-cluster contribution obtained from the 21-atom-cluster contribution by suppressing the second Si shell. Feature D has almost disappeared in the latter two cases, indicating that this peak arises from hydridization of the 3p states of the central atom with higher-neighbouring tetrahedral e orbitals (see the text).

the aim of achieving an understanding of these transition peaks, we show in figure 2(a) theoretical computations based on the X_α potential using different cluster sizes (5, 21, 57, and 109 atoms) and the $Z + 1$ final-state approximation. The clusters containing 5 to 109 atoms correspond to spheres of 1.6 to 7.0 Å radius around the photoabsorber atom with Si taken as the centre of the cluster. The 5-atom-cluster calculation already agrees well with the main absorption structures, stressing the importance of the tetrahedral symmetry of the silicon site. Since the spectrum should reflect the local empty p DOS, the feature B is therefore characteristic of the 1s-to-3p electronic transition in the local tetrahedral environment, while the wide structure F can be attributed mainly to MS inside the first oxygen shell. In figure 2(b), we show the results of a decomposed MS calculation made using the 5-atom cluster but suppressing the d bases of the central Si (curve (a)). Here, peak F has disappeared. This means that structure F arises from a dipole-allowed 1s-to-3d(t_2) transition due to the strong mixing of p and d orbitals in the final state. Considering the character table for T_d [44], one can see that the symmetry of the s silicon orbitals (a_1 orbitals) is described by the A_1 irreducible representation (IR), and the p and d_{xy}, d_{xz}, d_{yz} orbitals (t_2 orbitals) by T_2. The dipole-allowed electronic transitions are given by the direct IR product: $A_1 \rightarrow T_2$. On the other hand, since the irreducible representation e of T_d does not belong to the same 1s-to-3p channel, we cannot see another transition peak, related to e, in this small-cluster calculation as had been expected.

When the cluster contains 21 atoms, including the central Si atom, its four nearest O atoms, the four Si atoms in the outer shell, and twelve oxygen atoms that provide a tetrahedral environment for these four Si, a well-defined new peak labelled D appears. In the language of molecular-orbital (MO) theory, this peak can be attributed to central Si 3p states hybridized with e orbitals of outer-neighbouring tetrahedra formed by the second Si shell and 12 oxygen atoms. We verify this assignment by presenting another two different calculations in figure 2(b): for a 9-atom cluster (Si + 4O + 4Si) (curve (b)) and a 17-atom cluster obtained by suppressing the second Si shell from a 21-atom cluster (curve (c)). Neither of these shows the feature D, unlike the 21-atom-cluster result in the left-hand panel, due to the lack of a medium-range tetrahedral environment in these two atomic models. When the cluster size increases further, the calculated spectra reveal several fine structures. All features observed in the experimental spectrum are very well reproduced in the last large-cluster calculation (109 atoms), not only as regards the relative intensities, but also as regards the energy separations. This indicates that a 109-atom cluster is sufficient for describing bulk properties, and that the higher-neighbouring tetrahedral orbitals interact with each other and cause the molecular orbitals to overlap, forming extended energy bands and modifying their energy position. It is also clear that the 21-atom form used by Tanaka *et al* [25] is not good enough to describe all of the transition features.

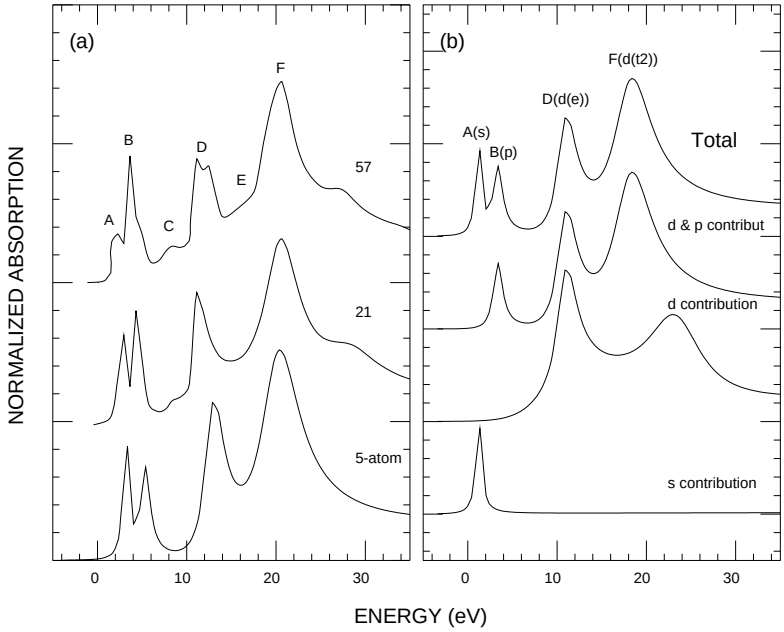

Figure 3. Panel (a): theoretical XANES spectra at the Si $L_{2,3}$ edges for α-SiO_2 for various cluster sizes (5, 21, and 57 atoms). Panel (b): the decomposition of the 5-atom-cluster MS calculation at the $L_{2,3}$ edges into s-like, d-like, and pd-like final states (emission channels) in α-SiO_2. It is clear that peak A corresponds to A_1(s), B to T_2(p), D to E(d), and F to T_2(d).

4.2. Si $L_{2,3}$ edges

The Si $L_{2,3}$-edge XANES spectrum is shown in figure 1(b). It contains six very pronounced transition peaks, A–F. The detailed MS simulations are shown in figure 3(a); they were

obtained by using an X_α potential and three different atomic clusters (5, 21, 57 atoms). The overall shape (peaks A, B, D, and F) is reproduced in the first 5-atom model calculation, indicating that these peaks arise from short-range interactions of Si with the first oxygen shell. Indeed, starting from initial p states (T_2 in T_d symmetry), the direct-product rule shows that the transitions $T_2 \rightarrow A_1$, $T_2 \rightarrow T_2$, $T_2 \rightarrow E$ are dipole allowed. We show a related decomposition of the Si $L_{2,3}$-edge XANES calculation into s-like, d-like, and pd-like final-state transitions in figure 3(b). It shows clearly that feature A corresponds to the p-to-s transition $T_2 \rightarrow A_1(s)$; peak B is attributed to a p–p transition, allowed in tetrahedral symmetry ($T_2 \rightarrow T_2(p)$); and the $p \rightarrow d(e)$ ($T_2 \rightarrow E$) and $p \rightarrow d(t_2)$ ($T_2 \rightarrow T_2$) transitions are responsible for the peaks D and F, respectively. It was not necessary to arbitrarily add the K-edge cross section to the $L_{2,3}$ ones as Hansen *et al* did [45]. The local environment of the silicon atom therefore causes the four main structures of the Si L edge. The agreement is excellent when the cluster includes 57 atoms, and even the weak structures C and E are reproduced in the calculated spectrum, confirming again that they arise from long-range interaction like those for the Si K edge. Since in our theory the absorption coefficient is nearly independent of the initial spin–orbit split edge, we are not able to reproduce the splitting of peak A that was shown in figure 1(b).

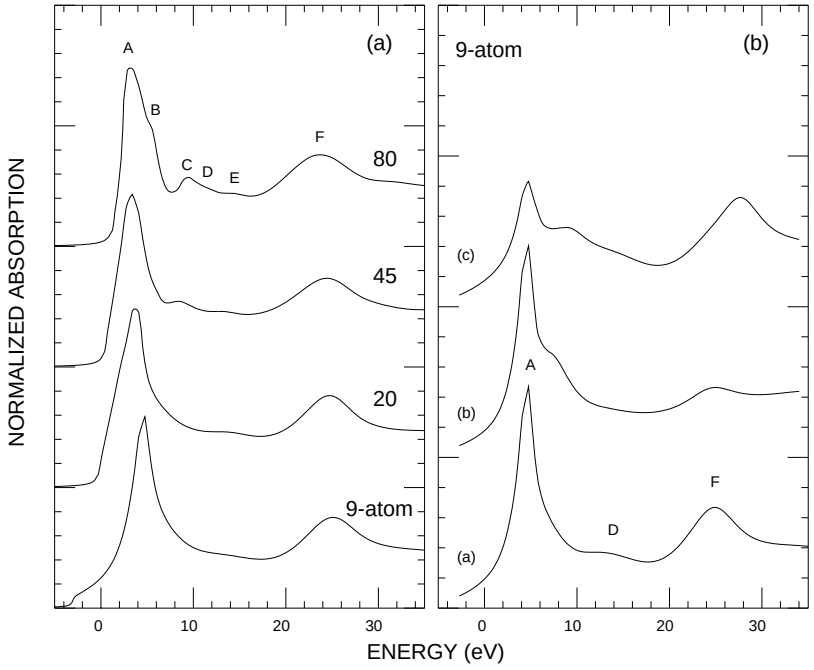

Figure 4. Panel (a): theoretical XANES spectra at the O K edge for α-SiO_2 for various cluster sizes (9, 20, 45, and 80 atoms). Panel (b): the 9-atom-cluster MS calculation for the O K edge. Curve (a): the normal cluster calculation; curve (b): taking into account only the sp-orbital contributions of outer-shell Si tetrahedra; peak B is almost constant but peaks D and F decrease substantially, indicating that the white line is mainly due to the hybridization of 2p states with Si sp states and D and F to the hybridization of 2p with Si d orbitals; curve (c): taking into account only the d-orbital contribution of the outer Si atoms; the behaviour is opposite to that of curve (b), demonstrating again the origin of peaks B, D, and F, as argued above.

4.3. The O K edge

Six spectral structures appear in the O K-edge XANES spectrum of α-SiO_2 as shown in figure 1(c): the threshold first shows an intense and broad white line constituted by at least two contributions (peaks A and B) followed by the three weak peaks, C, D, and E, and the broad structure F. In figure 4(a) we show the results of MS calculations of the O K-edge spectra made using four different cluster models (9, 21, 45, 80 atoms). The first cluster calculation (central O+2Si+6O) gives the general shape of the experimental spectrum. The first peak A is attributed to a resonance arising from MS inside the two adjacent tetrahedra, i.e. a constructive interference of all of the possible scattering paths inside the cluster. In the language of MO theory, feature A can be attributed to oxygen 2p states hybridized with Si 3s and 3p states [46]. In order to verify its origin, we show in figure 4(b) the results of a decomposed analysis made using the 9-atom cluster. Curve (a) is the same as the lowest curve in the left-hand panel; curve (b) is the contribution obtained by suppressing the d-like bases of the outer Si tetrahedra; the white line remains as in curve (a), but peaks D and F have almost disappeared, indicating that they largely arise from oxygen 2p states hybridized with the Si d molecular orbitals e and t_2. In the same way, when we suppress the s-like and p-like bases of Si atoms, the intensity of the white line decreases dramatically (see curve (c)), showing that there is a strong interaction between oxygen 2p and silicon 3s and 3p orbitals in this energy range. The extensive spread in energy and strong interaction with silicon for the entire conduction band of the oxygen 2p states is an indication of significant covalency in α-SiO_2. Other structures present in the experimental spectrum do indeed appear upon increasing the cluster size for the calculation by including the successive shells of neighbours.

4.4. The core-hole effect

Since the x-ray absorption process causes a core hole to be left in the final state after the electronic transition, core-hole potential effects can in principle distort the experimental spectrum considerably from the ground-state (GS) electronic structure. Many studies [24, 27, 47–52] of XAS for various systems, especially for compounds of light elements such as Al and Si, have shown recently that the core-hole potential has a profound influence on the XAS spectrum. Thus an understanding of the nature of the modification of the electronic structure by a core hole becomes absolutely essential for analysing the detailed electronic structure of materials.

In figure 5 we present the results of MS calculations based on two different final-state potentials. In one case we calculated the theoretical spectra on the basis of the $Z + 1$ approximation which accounts for the core-hole potential in the final state; in the other case we assumed that the final-state potential is the same as the GS potential. The left-hand panel of figure 5 shows the results of the two calculations for the Si K edge, while those for the Si $L_{2,3}$ edges and O K edge are shown in the middle and right-hand panels, respectively. As is clearly shown in the left-hand panel for the Si K edge, the absence of the core hole produced a very drastic change of the absorption spectrum—not only was there a shift of about 3.0 eV towards higher energy (opposite to the shifting towards lower energy shown by the dotted line), but also the calculated fine structures became much more distinct from the experimental ones. Our finding agrees well with those of Kortboyer *et al* [49] for Al alloys, Weijs *et al* [52] for transition metal silicates, Jollet and Noguera [24] for α-SiO_2, and other studies based on band-structure calculations.

The $L_{2,3}$ spectra as shown in the middle panel are almost identical, except a slight

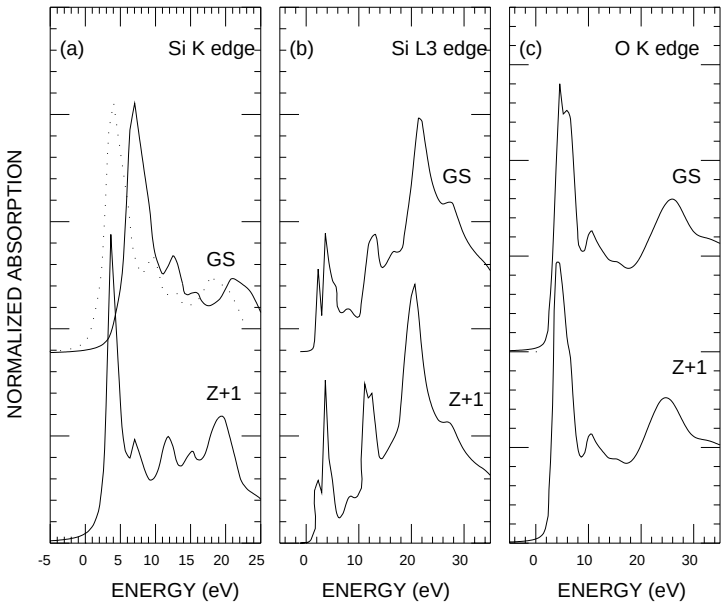

Figure 5. Comparison between two MS calculations for α-SiO_2, for the Si K, Si $L_{2,3}$, and O K edges, made using two different final-state potentials: the $Z+1$ final-state potential (lower curve) and the ground-state (GS) potential (upper curve). For better comparison of the $Z+1$ and GS curves, the GS spectrum for the Si K edge is also shifted by about 3.0 eV towards lower energy (dotted line, left-hand panel).

change of the intensity of peak B, as expected, because the $Z+1$ approximation is not applicable for the L edges and, which could be even more important, 2p states are too shallow in energy to be relaxed during the transition process for light elements [34].

The results of the calculations based on two different potentials at the O K edge are the same as those shown in right-hand panel. This is not surprising, because the core hole is now situated at the oxygen site while the states in the unoccupied bands just above the Fermi level have most of their weight on the silicon site, so they should be rather insensitive to the core-hole potential on the oxygen.

The present results, especially those for the Si K edge, are at variance with those given in reference [25], where the partial DOS at the ground state agrees well with the fine structure of the experimental XANES in the range $\leqslant$30 eV. In more detail, the cluster (Si_5O_{16}) model considered was not sufficient in size, as already discussed above. Even considering the presence of the attractive potential in the final state due to the core hole, some spectral features cannot be reproduced, because they are dependent on the long-range effect. If one looks closely at the Si 3p DOS and O 2p DOS in reference [25], it is easy to see that neither of them fitted well with the experimental data—not only were they lacking some peaks, but also they poorly reproduced the relative intensities. The importance of long-range order is also emphasized by the observation that the calculated spectra given in reference [25], obtained with a 21-atom cluster, are less sensitive to the difference in SiO_4 tetrahedral linkage in Si and O K-edge XANES. As a consequence, we are led to believe that the core-hole potential effects are in fact important in the interpretation of the Si K-edge XANES spectrum, and, at the same time, one must consider the 'long-range' order to describe the final-state wave function.

5. Summary and conclusions

We have carried out a detailed theoretical and experimental investigation of Si K-, Si $L_{2,3}$-, and O K-edge XANES spectra for α-SiO_2. We have obtained excellent agreement between the experimental data and one-electron full MS calculations for these edges with a reasonable choice of α, the overlap factor, and the interstitial potential. All of the spectral transition features have been analysed in terms of electronic properties, the ligand-field character, and the site symmetry. It is shown that the local symmetry of the silicon sites governs the main structures of the spectra for the silicon and oxygen edges. Consideration of the tetrahedral symmetry of the silicon site provides the key points for achieving an understanding of the electronic structure of the conduction band. Moreover, the presence of specific fine structures in the spectra is not difficult to explain by taking into account the hybridization of molecular orbitals originating from different tetrahedral units, and they are characteristic of the long-range order in the solid. These results consistently indicate the fairly strong covalent contribution to the bonding in α-SiO_2. Furthermore, we have presented theoretical calculations, with the final-state potential being described in terms of the $Z+1$ approximation as well as in terms of the ground-state potential. All of these studies allow us to discern the influence of the core hole on the XANES spectral shape.

In conclusion, our combined study of XANES spectra at Si K, Si $L_{2,3}$, and O K edges in α-SiO_2 has allowed us to elucidate the origins of the spectral features. We have noticed that the effects of the attractive core-hole potential on the p-like conduction bands are more pronounced, and also argued against the claim made in reference [25] that the partial DOS at the GS agrees well with experimental fine structures. In some cases—for instance, with the limited experimental energy resolution in electron energy-loss spectroscopy—the core-hole potential may well not be necessary to improve the degree of agreement between theory and experiment, and it will be possible to interpret the gross features within the framework of GS conduction bands in such cases [51].

References

[1] Nucho R N and Madhukar A 1980 *Phys. Rev.* B **21** 1576
[2] O'Reilly E P and Robertson J 1983 *Phys. Rev.* B **27** 3780
[3] Nada R, Catlow C R A, Dovesi R and Pisani C 1990 *Phys. Chem. Minerals* **17** 353
[4] Pantelides S T and Harrison W A 1976 *Phys. Rev.* B **13** 2667
[5] Wiech G 1984 *Solid State Commun.* **52** 803
[6] Wiech G and Kurmaev E Z 1985 *J. Phys. C: Solid State Phys.* **18** 4393
[7] Li Y P and Ching W Y 1985 *Phys. Rev.* B **31** 2172
[8] Simunek A, Vackar J and Wiech G 1993 *J. Phys.: Condens. Matter* **5** 867
[9] Xu Y N and Ching W Y 1991 *Phys. Rev.* B **44** 11 048
[10] Cherlov G B, Friedman S P, Kurmaev E Z, Viech G and Gubanov V A 1987 *J. Non-Cryst. Solids* **94** 276
[11] Binggeli N, Troullier N, Martins J L and Chelikowsky J R 1991 *Phys. Rev.* B **44** 4771
[12] Brown F C, Bachrach R Z and Skibowski M 1977 *Phys. Rev.* B **15** 4781
[13] Nithianandam V J and Schnatterly S E 1988 *Phys. Rev.* B **38** 5547
[14] Baba Y, Yamamoto H and Sasaki T A 1993 *Phys. Rev.* B **48** 10 972
[15] Nagashima N, Nakano A, Odata K, Tamura M, Sugawara K and Hayakawa K 1993 *Phys. Rev.* B **48** 18 257
[16] Li D, Bancroft G M, Kasrai M, Fleet M E, Feng X H, Tan K H and Yang B X 1993 *Solid State Commun.* **87** 613
[17] Marcelli A *et al* 1985 *J. Physique Coll.* **46** C8 107
[18] Lagarde P, Flank A M, Tourillon G, Liebermann R C and Itie J P 1992 *J. Physique* I **2** 1043
[19] Fuggle J C and Inglesfield J E (ed) 1992 *Unoccupied Electronic States (Springer Topics in Applied Physics 69)* (Berlin: Springer)
[20] Azizan M, Baptist R, Brenac A, Chauvet G and Nguyen Tan T A 1987 *J. Physique* **48** 81

[21] Azaroff L V and Peasa D M 1974 *X-ray Spectroscopy* ed L V Azaroff (New York: McGraw-Hill)
[22] Müller J E, Jepsen O and Wilkins J W 1982 *Solid State Commun.* **42** 365
Müller J E and Wilkins J W 1984 *Phys. Rev.* B **29** 4331
[23] Fowler W B, Schneider P M and Calabrese E 1978 *The Physics of SiO_2 and its Interfaces* ed S T Pantelides (London: Pergamon) p 70
[24] Jollet F and Noguera C 1993 *Phys. Status Solidi* b **179** 473
[25] Tanaka I, Kawai J and Adachi H 1995 *Phys. Rev.* B **52** 11 733
[26] Briois V, Sainctavit P and Flank A M 1993 *Japan. J. Appl. Phys.* **32** 52
[27] Chaboy J, Benfatto M and Davoli I 1995 *Phys. Rev.* B **52** 10 014
[28] Wu Z Y, Seifert F, Poe B and Sharp T 1996 *J. Phys.: Condens. Matter* **8** 3323
[29] Bart F, Jollet F, Duraud J P and Douillard L 1993 *Phys. Status Solidi* b **176** 163
[30] Lee P A and Pendry J B 1975 *Phys. Rev.* B **11** 2795
[31] Natoli C R, Misemer D K, Doniach S and Kutzler F W 1980 *Phys. Rev.* A **22** 1104
Natoli C R and Benfatto M 1986 *J. Physique Coll.* **47** C8 11
Natoli C R, Benfatto M, Brouder C, Ruiz Lopez M Z and Foulis D L 1990 *Phys. Rev.* B **42** 1944
Tyson T A, Hodgson K O, Natoli C R and Benfatto M 1992 *Phys. Rev.* B **46** 5997
[32] Durham P J, Pendry J B and Hodges C H 1982 *Comput. Phys. Commun.* **25** 193
[33] Bianconi A 1988 *X-ray Absorption: Principles, Applications, Techniques of EXAFS, SEXAFS, XANES* ed R Prinz and D Koningsberger (New York: Wiley)
[34] Durham P J 1988 *X-ray Absorption: Principles, Applications, Techniques of EXAFS, SEXAFS, XANES* ed R Prinz and D Koningsberger (New York: Wiley)
[35] Lee P A and Beni G 1977 *Phys. Rev.* B **15** 2862
[36] Wu Z Y, Benfatto M and Natoli C R 1992 *Phys. Rev.* B **45** 531
Wu Z Y, Benfatto M and Natoli C R 1993 *Solid State Commun.* **87** 475
Wu Z Y, Marcelli A, Mottana A, Giuli G, Paris E and Seifert F 1996 *Phys. Rev.* B **54** 2976
[37] Mattheiss L 1964 *Phys. Rev.* A **134** 970
[38] Clementi E and Roetti C 1974 *At. Data Nucl. Data Tables* **14** 177
[39] Fuggle J C and Inglesfield J E 1992 *Unoccupied Electronic States (Springer Topics in Applied Physics 69)* (Berlin: Springer) appendix B, p 347
[40] Norman J G 1974 *Mol. Phys.* **81** 1191
[41] Cabaret D, Sainctavit P, Ildefonse P and Flank A 1996 *J. Phys.: Condens. Matter* **8** 3691
[42] Harp G R, Saldin D K and Tonner B P 1993 *J. Phys.: Condens. Matter* **5** 5377
[43] Sutherland D G J, Kasrai M, Bancroft G M, Liu Z F and Tan K H 1993 *Phys. Rev.* B **48** 14 989
[44] Figgis B N 1966 *Introduction to Ligand Fields* (New York: Wiley)
[45] Hansen P L, Brydson R and McComb D W 1992 *Microsc. Microanal. Microstruct.* **3** 213
[46] de Groot F M F, Grioni M, Fuggle J C, Ghijsen J, Sawatzky G A and Petersen H 1989 *Phys. Rev.* B **40** 5715
[47] Grunes L A 1983 *Phys. Rev.* B **27** 2111
[48] Fuggle J C 1987 *Phys. Scr.* T **17** 64
[49] Kortboyer S W, Grioni M, Speier W, Zeller R, Watson L M, Gibson M T, Schafers F and Fuggle J C 1989 *J. Phys.: Condens. Matter* **1** 5981
[50] Bianconi A, Del Sole R, Selloni A, Chiaradia P, Fanfoni M and Davoli I 1987 *Solid State Commun.* **64** 1313
[51] Weng X, Rez P and Sankey O F 1989 *Phys. Rev.* B **40** 5694
[52] Weijs P J W *et al* 1990 *Phys. Rev.* B **41** 11 899